frontiers | Frontiers in Earth Science

TYPE Original Research
PUBLISHED 27 January 2023
DOI 10.3389/feart.2022.1041249

OPEN ACCESS

EDITED BY
Dongliang Luo,
Northwest Institute of Eco-Environment and Resources (CAS), China

REVIEWED BY
Jing Luo,
Northwest Institute of Eco-Environment and Resources (CAS), China
Qionglin Li,
Southwest Jiaotong University, China

*CORRESPONDENCE
Jianguo Lu,
jianguog@swpu.edu.cn
Huohai Yang,
huohai38@163.com

SPECIALTY SECTION
This article was submitted to Cryospheric Sciences, a section of the journal *Frontiers in Earth Science*

RECEIVED 10 September 2022
ACCEPTED 23 November 2022
PUBLISHED 27 January 2023

CITATION
Lu J, Tan L, Yang H, Wan X, Wang Y and Yan Z (2023), Experimental study on the hydro-thermal-deformation characteristics of cement-stabilized soil exposed to freeze–thaw cycles. *Front. Earth Sci.* 10:1041249. doi: 10.3389/feart.2022.1041249

Experimental study on the hydro-thermal-deformation characteristics of cement-stabilized soil exposed to freeze–thaw cycles

Jianguo Lu[1,2]*, Liling Tan[1], Huohai Yang[3]*, Xusheng Wan[1], Yindong Wang[1] and Zhongrui Yan[1]

[1]School of Civil Engineering and Geomatics, Southwest Petroleum University, Chengdu, China, [2]State Key Laboratory of Frozen Soil Engineering, Northwest Institute of Eco-Environment and Resources, Chinese Academy of Sciences, Lanzhou, China, [3]Petroleum Engineering School, Southwest Petroleum University, Chengdu, China

The exploration of the hydro-thermal characteristics and deformation behaviors of cement-stabilized soils is important for the prevention and control of freeze–thaw damage in cold region engineering. This study used six groups of cement-stabilized soil samples with different cement contents (i.e., 3%, 6%, 9%, 12%, 15%, and 18%) to investigate the variations in soil temperature, volumetric unfrozen water content, deformation, freezing temperature, and dry density. The results showed that the temperatures of the cement-stabilized soil samples during the freezing and thawing processes can be categorized into three stages and that the freezing temperature decreased with increasing cement content. Moreover, the cement content and ambient temperature significantly affected the volumetric unfrozen water content of the cement-stabilized soil samples during the freeze–thaw cycles, and the soil temperatures corresponding to the peak hysteresis degree were relatively consistent with the freezing temperature. The residual volumetric unfrozen water content primarily depended not only on the cement content but also on the freezing condition. Although the variations in volumetric unfrozen water contents during the freezing and thawing processes were similar, the ranges in temperature change differed significantly, particularly in the drastic phase transition zone. Additionally, adding cement into soils effectively inhibited deformation, mainly due to the dual positive effects of the liquid water reduction owing to hydration reaction and structure compaction owing to the filling of hydration products.

KEYWORDS

freeze–thaw cycles, cement-stabilized soil, soil temperature, volumetric unfrozen water content, deformation

1 Introduction

Owing to the rapid development of civil engineering constructions, several engineering infrastructures have been constructed in cold regions and permafrost areas, including the Qinghai–Tibet railway and highway (Cheng et al., 2008; Lu et al., 2019a), Sichuan–Tibet railway (Xue et al., 2021), Harbin Dalian high-speed railway (Tai et al., 2017), and Gonghe-Yushu highway (Pei et al., 2022), as well as tunnels (Zhang et al., 2017), embankment dams (Zhang et al., 2021), and canals (Li et al., 2015) in cold regions. The geological challenges in cold region engineering are extremely complex, particularly the effect of frost heave and thaw settlement on engineering durability. Therefore, reinforcement measures to strengthen the engineering properties of weak soils must be investigated. As a mixed geotechnical material that features low cost, high strength, and simple preparation, cement-stabilized soil is widely used in many civil engineering applications, such as expansive soil foundation improvement (Madhyannapu and Puppala, 2014), underground liquid natural gas storage (Yu et al., 2022), fine-grained lateritic soil modification for pavement foundation layers (Mengue et al., 2018), slope stabilization in swelling soils (Daraei et al., 2018), and soft foundation reinforcement (Kang et al., 2017; Yi et al., 2018; Wang et al., 2022).

Generally, adding materials such as fibers (Tang et al., 2010; Malekzadeh and Bilsel, 2014; Wei et al., 2018; Akbari et al., 2021; Lu et al., 2022a), mineral admixtures (Chew et al., 2004; Consoli et al., 2011; Mardani-Aghabaglou et al., 2015; Behnood, 2018; Bunawan et al., 2018; Wei et al., 2018; Luis et al., 2019; Zhang et al., 2019; Lu et al., 2022a), and nano-materials (Taha, 2009; Taha and Taha, 2012; Meng et al., 2017; Behnood, 2018; Akbari et al., 2021; Wang et al., 2021) to soils is considered an effective measure to improve the durability of geotechnical materials in engineering applications. The overall performances of soils modified with additives have been investigated extensively. Various fibers, including plant (e.g., rice straw, wheat straw, palm fiber, bagasse fiber, bamboo fiber, sisal fiber, coir fiber, and jute fiber) and synthetic (e.g., nylon fiber, polyester fiber, polypropylene fiber, glass fiber, basalt fiber, alcohol fiber, and PVA fiber) fibers have been extensively used to improve the geotechnical parameters of soil by reducing crack propagation and mass loss, increasing shear and tensile strengths, and enhancing ductility (Tang et al., 2010; Malekzadeh and Bilsel, 2014; Wei et al., 2018; Akbari et al., 2021; Lu et al., 2022a). Additionally, mineral admixtures, including lime, cement, fly ash, slag, and metakaolin, have been widely applied to enhance soil properties. Among them, cement and lime are the two most typically used soil stabilization agents in engineering applications (Behnood, 2018). Adding cement and fly ash to soils can increase the setting time and decrease the viscosity. Moreover, fresh mixes show good homogeneity and stability, thus providing good performance (Chew et al., 2004; Bunawan et al., 2018). Factors including porosity, cement content, and volumetric water content significantly affect the mechanical properties of cement-stabilized soils (Consoli et al., 2011). Additionally, owing to their small particle size, high specific surface area, and reactivity, various nano-materials (e.g., nano-zeolite, nano-SiO_2, nano-Al_2O_3, nano-TiO_2, nano-$CaCO_3$, nano-CuO, nano-clay, and carbon nanotubes) are typically used to enhance the properties of treated soils (Taha, 2009; Taha and Taha, 2012; Mardani-Aghabaglou et al., 2015; Meng et al., 2017; Behnood, 2018; Akbari et al., 2021; Wang et al., 2021). The overall performance of nanoparticle-treated soils shows significant improvement within the optimum range of nano-material content, including improved mechanical properties and decreased plasticity (Taha, 2009), reduced swelling and shrinkage strains (Taha and Taha, 2012), and enhanced corrosion resistance (Wang et al., 2021). Moreover, polymers, including various polymer precursors, emulsions, resins, and biopolymers, have been used to improve the mechanical properties, reduce hydraulic conductivity, and enhance the pore structures of treated soils (Al-Khanbashi and Abdalla, 2006; Mujah et al., 2015; Rezaeimalek et al., 2017). The findings of previous studies have suggested that adding materials to soils can significantly improve the bearing capacity and stability of geotechnical materials, particularly for cement-stabilized soils, although many of these studies primarily focused on the mechanical and hydraulic properties of treated soils. In cold regions, water migration and redistribution significantly affect the hydro-thermal characteristics and deformation behaviors (Lu et al., 2019a; Lu et al., 2019b; Lu et al., 2021), which might consequently affect the mechanical properties of soils (Lai et al., 2014).

Yu et al. (2022) studied the mechanical, physical, and thermal characteristics of cement-stabilized soil surrounding an underground LNG system exposed to freeze–thaw cycles, concluding that the deformation, thermal conductivity, and volume expansion of the cement-stabilized soil were superior to those of untreated soil; thus, cement-stabilized soil can be used to prevent potential damage to adjacent facilities. Lu et al. (2020) explored the mechanical properties and deformation behavior of cement-treated expansive soils and demonstrated that the cement-treated expansive soil was less sensitive to moisture. The addition of cement changes the freeze–thaw performance of expansive soils, by increasing their compressive strength and resilient modulus, reducing swelling and shrinkage deformations triggered by freeze–thaw cycles, and diminishing the strain at failure. Ding et al. (2018) investigated the mechanical properties of clay stabilized with cement and polypropylene fiber under freeze–thaw cycles and found that cement-stabilized soils showed volumetric shrinkage, whereas soil modified with cement and polypropylene fiber showed volumetric expansion. The unconfined compressive strength and stress-strain curves changed significantly in the first freeze–thaw cycle and then remained almost unchanged with additional freeze–thaw cycles. However, these studies primarily focused on the mechanical

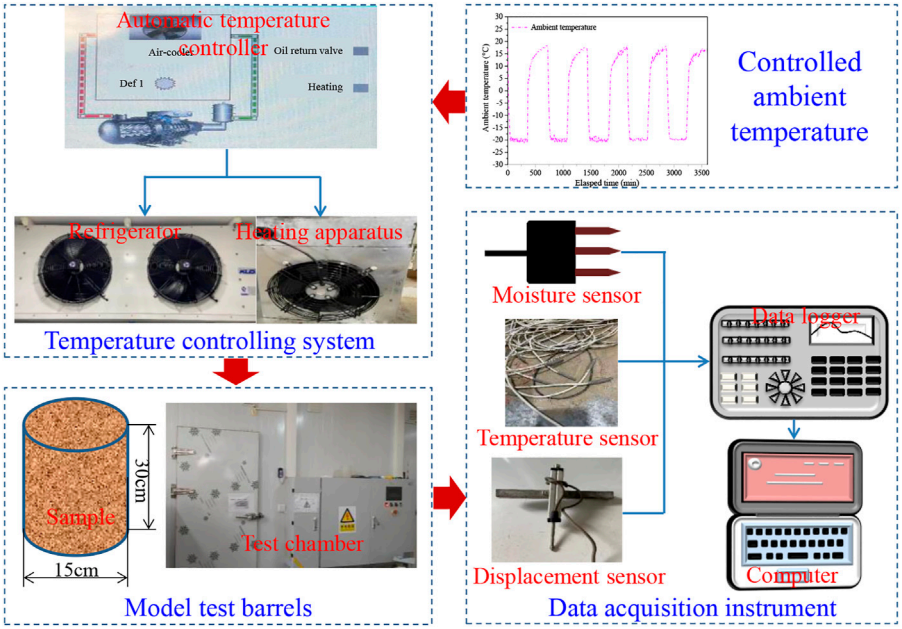

FIGURE 1
Schematic illustration of the experimental apparatus and controlled ambient temperature.

properties of cement-stabilized soils, and the variations in the hydro-thermal characteristics and deformation behaviors of cement-stabilized soils exposed to freeze–thaw cycles are rarely investigated. Permafrost areas and seasonally frozen ground constitute approximately 22.4% and 55.0% of the Earth's land area, respectively, which is similar to the distribution in China (Qiu et al., 1994). Hence, geotechnical materials are inevitably exposed to freeze–thaw cycles, and the frost heave and thaw settlement of frozen soils significantly affect the construction and maintenance of geotechnical engineering. Freeze–thaw cycles significantly affect the hydro-thermal-deformation characteristics of soils, and some soil properties vary considerably during the freezing and thawing processes, including thermal conductivity (Zhang et al., 2018a; Bi et al., 2020; Lu et al., 2021), matric suction (Lu et al., 2018), volumetric unfrozen water content (Zhang et al., 2018b; Lu et al., 2022b), deformation, and dry density (Qi et al., 2006; Qi et al., 2008; Lu et al., 2018; Lu et al., 2022b). Therefore, the hydro-thermal-deformation characteristics of cement-stabilized soil exposed to freeze–thaw cycles must be investigated.

The present study conducted a series of experiments to investigate the hydro-thermal-deformation characteristics of cement-stabilized soil exposed to freeze–thaw cycles. Six groups of cement-stabilized soil samples with different cement contents (i.e., 3%, 6%, 9%, 12%, 15%, and 18%) were prepared and then subjected to freeze–thaw cycle tests. The temperature, volumetric unfrozen water content, and deformation of the cement-stabilized soil samples were monitored during the freezing and thawing processes. Subsequently, the relationships among soil temperature, volumetric unfrozen water content, and deformation were analyzed. These findings provide an improved understanding of the variations in the hydro-thermal characteristics and deformation behaviors of cement-stabilized soil to help prevent or control freeze–thaw damage in cold region engineering.

2 Experimental design

2.1 Experimental apparatus

Figure 1 shows a schematic illustration of the experimental apparatus, which comprised three components: a temperature control system, model test barrels, and a data acquisition system. The temperature control system consisted of a compressor, an evaporator, refrigerant circulation pipelines, and an automatic temperature controller that maintained the experimental ambient environment at the desired temperature. The model test barrels had inner diameters of 15 cm and heights of 30 cm. The bottoms of the barrels were insulated with 5-cm-thick rigid polyurethane sheets to freeze the samples from the top and radial directions.

The data acquisition system comprised a data logger and sensors (temperature, deformation, and volumetric unfrozen water content sensors). The temperature sensor was a

TABLE 1 Physical properties of the soil.

Soil property	Value
Specific gravity	2.71
Liquid limit (gravimetric water content) (%)	31.64
Plastic limit (gravimetric water content) (%)	16.72
Plasticity index	14.92

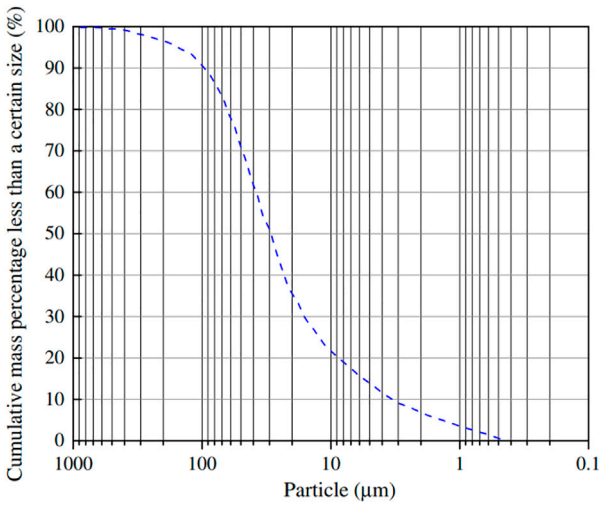

FIGURE 2
Grain-size distribution of silty clay.

thermistor temperature sensor with a temperature measurement ranging from −30°C to 30°C and a temperature accuracy of ±0.05°C. The temperature sensors were embedded at depths of 5 cm (T1) and 10 cm (T2) from the top. The deformation sensor was based on a linear displacement sensor with a precision of ±0.1 F.S. (full scale) and was arranged on the tops of the samples. The volumetric unfrozen water content sensor, which featured three 5.2-cm-long probes, was based on the principle of frequency domain reflection, with a sensor precision of ±0.03 m^3/m^3. The volumetric unfrozen water content of the soil was calculated based on its dielectric permittivity, which indirectly reflected the frequency of electromagnetic waves. The volumetric unfrozen water content sensor was placed in the middle of the samples. Based on the calibration of the volumetric unfrozen water content sensor for the soil, a third-order polynomial equation was used to calculate the volumetric unfrozen water content (Topp et al., 1980; Lu et al., 2022b), as follows:

$$\theta_u = 8.07 \times 10^{-6}\varepsilon^3 - 8.57 \times 10^{-4}\varepsilon^2 + 3.46 \times 10^{-2}\varepsilon - 8.36 \times 10^{-2}, \quad (1)$$

TABLE 2 Main chemical compositions of the Portland cement used in the experiments.

Chemical composition	Mass ratio (*wt.* %)
CaO	62.32
SiO_2	21.04
Al_2O_3	5.53
Fe_2O_3	3.98
SO_3	2.62
MgO	1.75
K_2O	0.78

where θ_u and ε are the volumetric unfrozen water content and dielectric permittivity of the soil, respectively.

All sensors were connected to a data logger connected to a computer. The data acquisition interval was 5.0 min.

2.2 Experimental procedure

Silty clay was derived from the soil from Gansu Province through a series of treatment procedures (drying, crushing, and sieving) to eliminate particles >2 mm. The physical properties and grain-size distributions of the silty clay are shown in Table 1 and Figure 2, respectively. Ordinary graded 42.5 Portland cement, produced by Lafarge Cement Co., Ltd. in Sichuan Province, was used as a stabilization agent. The main chemical composition of Portland cement is listed in Table 2. According to the Chinese national standard of specifications for the mix proportion design of cement soil (JGJ/T 233-2011, 2011), the cement content in cement-stabilized soil is defined as the ratio of dried cement mass to dried soil mass, as follows:

$$\xi = (m_c/m_s) \times 100\%, \quad (2)$$

where ξ is the cement content, and m_c and m_s are the masses of dried cement and dried soil, respectively.

Six cement-stabilized soil samples with cement contents of 3%, 6%, 9%, 12%, 15%, and 18% were prepared, the mix proportions of which are listed in Table 3. The initial volumetric water content of the cement-stabilized soil sample with a cement content of 3% (N01) was 14.8%. The other samples (N02, N03, N04, N05, and N06) had an initial volumetric water content of 25.8%.

The required cement, soil, and distilled water were weighed and the cement-stabilized soil samples were prepared as follows: first, the cement and soil were mixed to a uniform consistency. Next, water was added to the mixture, and the latter was stirred in a forced mixer for 30 s to create a homogeneous paste. The mixture was then compacted into a sample barrel using a

TABLE 3 Mixture proportions of cement-stabilized soil samples (%).

Sample no.	Cement content (%)	Initial water content (%)	Dry density (g/cm^3)	Number of freeze–thaw cycles
N01	3	14.8	1.70	5
N02	6	25.8	1.70	
N03	9	25.8	1.70	
N04	12	25.8	1.70	
N05	15	25.8	1.70	
N06	18	25.8	1.70	

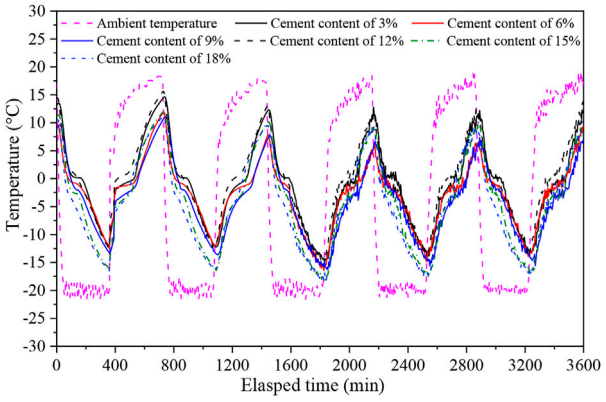

FIGURE 3
Variations in soil temperature during the freeze–thaw cycles.

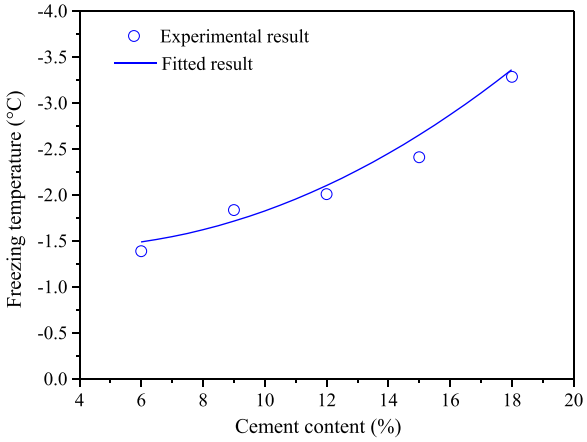

FIGURE 4
Freezing temperature of cement-stabilized soil samples with different cement contents.

hammer to achieve the target dry density. Next, the samples were sealed in a plastic bag for 24 h at an ambient temperature of 20 ± 2°C to ensure adequate moisture redistribution. Before the experiment, the prepared cement-stabilized soil samples were placed in a refrigerator at an ambient temperature of 20°C for 7 days to ensure even distribution of the moisture and soil temperature and full hydration reaction between the cement and water in the soil. Subsequently, freeze–thaw cycle tests were performed. Each freeze–thaw cycle lasted for 12 h, in which the ambient temperature was decreased from 20°C to −20°C for 1 h, maintained at −20°C for 5 h (cooling process), increased from −20°C to 20°C for 1 h, and maintained at 20°C for 5 h (warming process). A total of six freeze–thaw cycles were performed for the samples.

3 Results and discussions

3.1 Variations in soil temperature

Figure 3 shows the variations in soil temperature for the cement-stabilized soil samples during the freeze–thaw cycles. The soil temperatures during the freezing processes were categorized into three stages: rapid cooling, transient constant temperature, and cooling-freezing. The rapid cooling stage, i.e., the non-icing stage, occurred due to the rapid cooling of the samples. In this stage, no water phase change occurred and no ice crystals appeared in the samples. The transient constant temperature stage, i.e., the supercooling stage, was a metastable state during which the water in the cement-stabilized soil samples remained unfrozen even below the freezing temperature. The supercooling temperature of the cement-stabilized soil decreased with increasing initial cement content, except for the sample with a cement content of 12% (N04). As the freeze–thaw cycle progressed, the duration of the supercooling stage decreased, possibly due to the hydration reaction between the cement and water in the soil samples. During the cooling-freezing stage, the liquid water in the samples gradually froze. Similarly, the soil temperature during the warming processes was divided into three stages: rapid increase, relatively slow increase, and steady melting. The rapid increase stage of the soil temperature occurred due to a rapid increase in the ambient temperature.

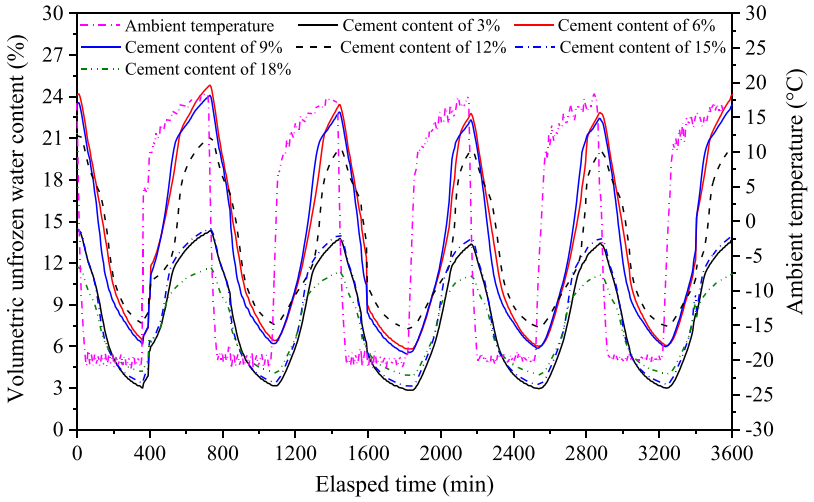

FIGURE 5
Variations in the volumetric unfrozen water contents of cement-stabilized soil samples during the freeze–thaw cycles.

In the relatively slow increase stage, the ice in the samples rapidly melted, although the soil temperature gradually increased. Additionally, with increasing numbers of freeze–thaw cycles, the duration of the relatively slow increase stage decreased and the temperature range of soil samples in the thawing and freezing stages stabilized. This might have occurred due to the significant changes in the thermal parameters (primarily the volumetric heat capacity and thermal conductivity) and the pore structure of the cement-stabilized soil samples with increasing freeze–thaw cycles, owing to the hydration reaction between the cement and water and the effect of the freeze–thaw cycles on the pore structure of the samples.

3.2 Freezing temperatures of cement-stabilized soil samples

The freezing temperature of geotechnical materials used in cold region engineering must be determined to verify whether the materials are in a frozen or thawed state. Figure 4 shows the freezing temperatures of cement-stabilized soil samples with different cement contents. Under the same initial volumetric water content (25.8%), the freezing temperature of the cement-stabilized soil samples decreased with increasing cement content. This may be due to the dual effects of hydration reaction and pore action; the clinker minerals in cement, such as tricalcium silicate, dicalcium silicate, and tricalcium aluminate, underwent hydration and hydrolysis reactions with liquid water in the soil. Thus, some of the free water in the soils was converted to bound water, resulting in decreased free water content in the soil. Consequently, when a water-ice phase transition occurred, less latent heat was released and the freezing temperature decreased. Meanwhile, as the cement content increased, the cementation effect of cement in the soil decreased the size of the soil pores; thus, the freezing temperature of the cement-stabilized soil decreased with increasing cement content because the freezing of soil originated from the larger pores (Figure 4). Based on the regression analysis of the experimental data, the relationship between the freezing temperature and the cement content of the cement-stabilized soil can be expressed as follows:

$$T_f = -0.009\xi^2 + 0.06\xi - 1.524 \ (R^2 = 0.9764), \quad (3)$$

where ξ is the cement content of the cement-stabilized soil samples.

3.3 Variations in volumetric unfrozen water content

3.3.1 Effect of cement content on volumetric unfrozen water content

Figure 5 shows the variations in volumetric unfrozen water content of the cement-stabilized soil samples with an initial water content of 25.8% during the freeze–thaw cycles. The cement content and ambient temperature significantly affected the volumetric unfrozen water contents of the cement-stabilized soil samples during the freeze–thaw cycles. Cement-stabilized soil samples with low cement contents showed higher liquid water contents before the freeze–thaw cycles compared to those in samples with high cement content. This occurred due to the hydration reaction between the cement and liquid water in the

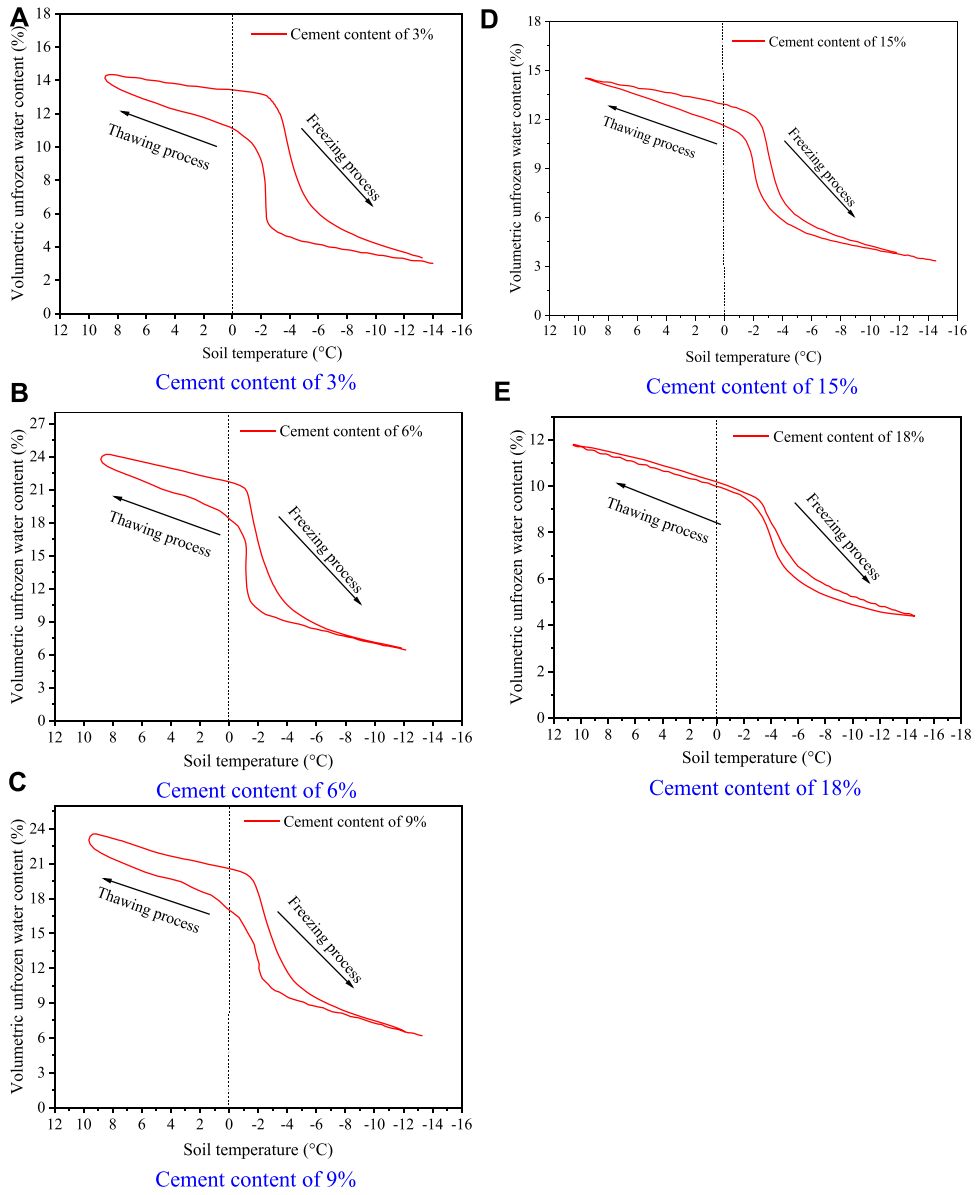

FIGURE 6
Hysteresis of the volumetric unfrozen water content of cement-stabilized soil samples in freezing and thawing processes.

soil and the formation of hydration products (e.g., CH gels and C-S-H crystals) before the freeze–thaw cycles (7 days), which resulted in a relatively compact structure. Consequently, the liquid water in the soil was consumed and the liquid water content decreased. The liquid water content before the freeze–thaw cycles in the cement-stabilized soil samples with cement contents of 6% (N02), 9% (N03), 12% (N04), 15% (N05), and 18% (N06) decreased from 25.8% to 24.09%, 23.48%, 21.18%, 14.50%, and 11.73%, respectively (Figure 5).

Figure 5 also shows that the volumetric unfrozen water content of the cement-stabilized soil samples decreases (increased) with decreased (increased) ambient temperature during the freezing and thawing processes. The residual volumetric unfrozen water content of the cement-stabilized soil samples, as an important index for evaluating the frost characteristics of geotechnical materials in cold regions, depends on both the cement content and its freezing conditions (Figure 5). Additionally, the freeze–thaw cycles slightly affected the total liquid water and residual volumetric unfrozen water contents of the cement-stabilized soil samples. The total liquid water content of the sample with a cement content of 15% changed from 14.5% (before the freeze–thaw test)

to 14.29% (first freeze–thaw cycle), 14.08% (second freeze–thaw cycle), 13.63% (third freeze–thaw cycle), 13.51% (fourth freeze–thaw cycle), and 14.13% (fifth freeze–thaw cycle). Meanwhile, the residual volumetric unfrozen water content varied from 3.0% to 4.0% during the fifth freeze–thaw cycle (Figure 5). These findings indicated that a slight hydration reaction occurred during the freezing and thawing processes.

3.3.2 Hysteresis of the volumetric unfrozen water content

Figure 6 shows the hysteresis of the volumetric unfrozen water content for the cement-stabilized soil samples during the freezing and thawing processes. Obvious hysteresis was observed in the volumetric unfrozen water content between the freezing and thawing processes, with a higher volumetric unfrozen water content of the cement-stabilized soil samples during the freezing process compared to that during the thawing process. Generally, similar variations in volumetric unfrozen water content were observed during the freezing and thawing processes; i.e., the volumetric unfrozen water content first slowly decreased, then rapidly decreased, and slowly decreased again before stabilizing. However, the ranges of the temperature changes of the volumetric unfrozen water contents differed significantly. During the freezing process, the soil temperature corresponding to the drastic phase transition zone ranged from −1°C to −6°C, during which stage the clear transformation of the water-ice caused a rapid reduction of the volumetric unfrozen water content and significant variations in the soil structure. Compared to the phase transition zone of silty clay, the drastic phase transition zone of the cement-stabilized soil samples showed a wider temperature range and a lower initial temperature (Zhang et al., 2018a; Lu et al., 2022b), possibly because the hydration reaction between the cement and water in the soil reduced the amount of liquid water and the hydration products occupied the pores, thus resulting in a compacted structure of the cement-stabilized soil samples. Indeed, freezing originated from the macro-pores of the geotechnical materials, leading to a wider temperature range and lower initial temperature in the drastic phase transition zone. The soil temperature corresponding to the drastic phase transition zone during the thawing process ranged from −4°C to 0°C.

In the drastic phase transition zone, the change slope of the volumetric unfrozen water content for the cement-stabilized soil samples with a lower cement content was greater than that for the cement-stabilized soil samples with a higher cement content owing to differences in the amount of liquid water and macro-pores in the samples (Figure 6). Additionally, as the cement content increased, the interval and difference in the volumetric unfrozen water content between the freezing and thawing processes decreased (Figure 6).

To quantitatively investigate the characteristics of the hysteresis of the volumetric unfrozen water content for the cement-stabilized soil samples, an important index; i.e., the hysteresis degree of the volumetric unfrozen water content, $\Delta\theta$, was proposed,

$$\Delta\theta = \theta_f - \theta_t, \tag{4}$$

where θ_f and θ_t are the volumetric unfrozen water content at the same time during the freezing and thawing processes, respectively.

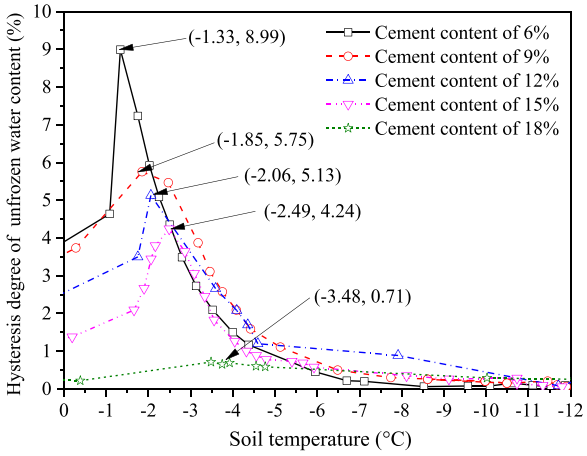

FIGURE 7
Hysteresis degrees of volumetric unfrozen water content for cement-stabilized soil samples with different cement contents.

Figure 7 shows the hysteresis degree of the volumetric unfrozen water content for the cement-stabilized soil samples with different cement contents. Regardless of the cement content, as the soil temperature decreased, the hysteresis degree of the volumetric unfrozen water content first increased, and then decreased from the peak value and approached zero. The peak value occurred within the range of the drastic phase transition zone. For cement-stabilized soil samples with cement contents of 6%, 9%, 12%, 15%, and 18%, the soil temperatures corresponding to the peak value were −2.53°C, −1.33°C, −1.85°C, −2.49°C, and −3.48°C, respectively, which were relatively consistent with the freezing temperatures (Figure 7). Moreover, under the same initial volumetric water content (25.8%), the peak values of the hysteresis degrees of the volumetric unfrozen water content decreased with increasing cement content; for instance, the peak hysteresis degrees for samples with cement contents of 6%, 9%, 12%, 15%, and 18% were 8.99%, 5.75%, 4.24%, 0.71%, and 0.71%, respectively (Figure 7). As the cement content increased, more liquid water was consumed owing to the hydration reaction, and the soil structures were compacted with more micro-pores, which resulted in a slight difference in volumetric unfrozen water content between the freezing and thawing processes.

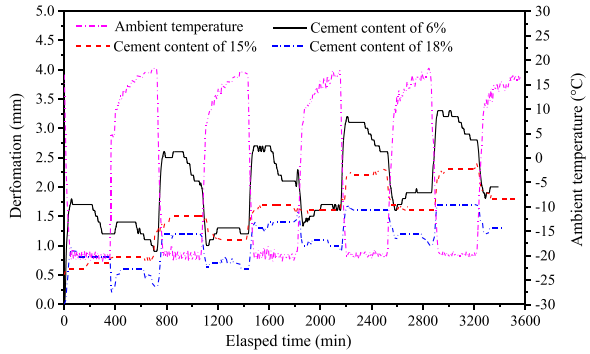

FIGURE 8
Variations in the deformation of cement-stabilized soil samples with different cement contents.

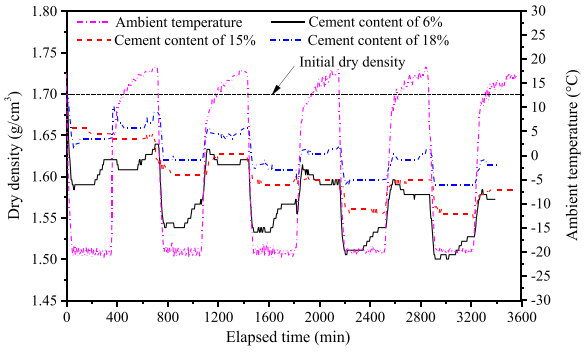

FIGURE 9
Variations in the dry density of cement-stabilized soil samples with different cement contents.

3.4 Variations in deformation

Figure 8 shows the variations in the deformation of the cement-stabilized soil samples with cement contents of 6%, 15%, and 18%. During the cooling processes, when the soil temperature was below the freezing temperature and the ambient temperature continuously decreased, frost heave occurred due to the water-ice phase transition. During the warming processes, owing to the immersion of heat energy, the frozen soil melted, and thaw settlement appeared. Under the same freeze–thaw cycles, cement-stabilized soil samples with high cement content showed less deformation compared to that in samples with low cement content. The deformation of the sample with a cement content of 18% was the lowest, followed by those with cement contents of 15% and 6%. This finding occurred because the soil samples with high cement content had less liquid water and featured compacted structures. Furthermore, after each freeze–thaw cycle, the samples showed a net deformation greater than zero, which indicated an increased volume of the cement-stabilized soil samples (Figure 8).

Additionally, the freeze–thaw cycles significantly affected the variation in deformation, particularly in the first freeze–thaw cycle. The maximum frost heave and net deformation increased and stabilized as the number of freeze–thaw cycles increased. After the fifth freeze–thaw cycle, the maximum frost heaves of the soil samples with cement contents of 6%, 15%, and 18% were 3.3 mm, 2.3 mm, and 1.7 mm, respectively, and the net deformations were 2.0 mm, 1.8 mm, and 1.3 mm, respectively (Figure 8). Furthermore, adding cement to the soil effectively inhibited the deformation, including frost heave and thaw settlement. For the same initial volumetric water content, the higher the cement content, the more effective the deformation inhibition. This might be due to the dual positive effects of the liquid water reduction owing to the hydration reaction and the compacted structure owing to the filling of hydration products, which resulted in lower swelling stresses during the freezing and thawing processes.

To further investigate the characteristics of the cement-stabilized soils exposed to freeze–thaw cycles, the dry density of the soil samples during the freezing and thawing processes was calculated by considering the frost heave and thaw settlement,

$$\rho_d = \frac{4m_s}{\pi d^2 (h_0 + \Delta h)}, \quad (5)$$

where m_s is the mass of the dry materials including cement and soil; d is the diameter of the cement-stabilized soil samples; and h_0 and Δh are the initial height and deformation of the cement-stabilized soil samples, respectively.

Figure 9 shows the variations in dry density for the cement-stabilized soil samples with different cement content. During the freezing processes, the dry densities decreased with decreasing ambient temperature and increased with increasing ambient temperature during the thawing processes. However, after each freeze–thaw cycle, the dry densities decreased compared to the initial dry density, which indicated a downward trend in the dry densities of the cement-stabilized soil samples with increasing numbers of freeze–thaw cycles (Figure 9). Moreover, the freeze–thaw cycles significantly affected the variations in dry densities, especially in the first freeze–thaw cycle. The dry densities of cement-stabilized soil samples with higher cement content decreased faster than those with lower cement content. After three freeze–thaw cycles, the effect of freeze–thaw cycles on the dry densities of the cement-stabilized soil samples weakened, and the dry densities gradually stabilized. For instance, the dry densities of the cement-stabilized soil samples with cement contents of 6%, 12%, and 18% decreased from 1.7 g/cm^3 to 1.57 g/cm^3, 1.58 g/cm^3, and 1.62 g/cm^3, respectively. Thus, freeze–thaw cycles may loosen dense soils, although the hydration products can effectively occupy the macro-pores.

4 Conclusion

This study experimentally investigated the hydro-thermal-deformation characteristics of cement-stabilized soil exposed to freeze–thaw cycles. The following conclusion can be drawn:

1) The temperatures of the cement-stabilized soil samples during the freezing and thawing processes can be categorized into three stages. The supercooling temperature decreased as the initial cement content increased, and the duration of the supercooling stage decreased with increasing numbers of freeze–thaw cycles. In addition, the freezing temperature of the cement-stabilized soil samples decreased with increasing cement content.
2) The cement content and ambient temperature significantly affected the volumetric unfrozen water content of the cement-stabilized soil samples during the freeze–thaw cycles. The residual volumetric unfrozen water content mainly depended on both the cement content and freezing conditions. Although the variations in volumetric unfrozen water content during the freezing and thawing processes were similar, the ranges of temperature change differed significantly, particularly in the drastic phase transition zone.
3) As the cement content increased, the interval of volumetric unfrozen water content between the freezing and thawing processes decreased. The peak hysteresis degree of the volumetric unfrozen water content decreased with increasing cement content. Additionally, the soil temperatures corresponding to the peak value of the hysteresis degree were relatively consistent with the freezing temperature.
4) The freeze–thaw cycles significantly affected the variations in deformation and dry density, especially in the first freeze–thaw cycle. Adding cement to soils can effectively inhibit deformation; for the same initial soil water content, the higher the cement content, the more effective the deformation inhibition. This occurred primarily due to the dual positive effects of liquid water reduction owing to the hydration reaction and the compacted structure owing to the filling of the hydration products.

Data availability statement

The original contributions presented in the study are included in the article/Supplementary Material, further inquiries can be directed to the corresponding authors.

Author contributions

JL administered the project, organized the draft, revised the manuscript, and provided funding; LT conducted the experiment, collected the data, and plotted the figures; HY designed the experiment and revised the manuscript; XW edited the draft and provided funding; YW investigated the research status and conducted the experiments; and ZY performed the analysis.

Funding

This research was supported by the National Natural Science Foundation of China (Grant Nos. 42101136, 42271146), the Natural Science Foundation of Sichuan Province (Grant No. 2022NSFSC0429), the China Postdoctoral Science Foundation (Grant No. 2021M692697) and the State Key Laboratory of Frozen Soil Engineering (Grant No.SKLFSE202007).

Conflict of interest

The authors declare that the research was conducted in the absence of any commercial or financial relationships that could be construed as a potential conflict of interest.

Publisher's note

All claims expressed in this article are solely those of the authors and do not necessarily represent those of their affiliated organizations, or those of the publisher, the editors, and the reviewers. Any product that may be evaluated in this article, or claim that may be made by its manufacturer, is not guaranteed or endorsed by the publisher.

Supplementary material

The Supplementary Material for this article can be found online at: https://www.frontiersin.org/articles/10.3389/feart.2022.1041249/full#supplementary-material

References

Akbari, H. R., Sharafi, H., and Goodarzi, A. R. (2021). Effect of polypropylene fiber and nano-zeolite on stabilized soft soil under wet-dry cycles. *Geotext. Geomembranes* 49 (6), 1470–1482. doi:10.1016/j.geotexmem.2021.06.001

Al-Khanbashi, A., and Abdalla, S. W. (2006). Evaluation of three waterborne polymers as stabilizers for sandy soil. *Geotech. Geol. Eng. (Dordr).* 24 (6), 1603–1625. doi:10.1007/s10706-005-4895-3

Behnood, A. (2018). Soil and clay stabilization with calcium- and non-calcium-based additives: A state-of-the-art review of challenges, approaches and techniques. *Transp. Geotech.* 17, 14–32. doi:10.1016/j.trgeo.2018.08.002

Bi, J., Zhang, M. Y., Lai, Y. M., Pei, W. S., Lu, J. G., You, Z. L., et al. (2020). A generalized model for calculating the thermal conductivity of freezing soils based on soil components and frost heave. *Int. J. Heat Mass Transf.* 150, 119166. doi:10.1016/j.ijheatmasstransfer.2019.119166

Bunawan, A. R., Momeni, E., Armaghani, D. J., Nissa binti Mat Said, K., and Rashid, A. S. A. (2018). Experimental and intelligent techniques to estimate bearing capacity of cohesive soft soils reinforced with soil-cement columns. *Measurement* 124, 529–538. doi:10.1016/j.measurement.2018.04.057

Cheng, G. D., Wu, Q. B., and Ma, W. (2008). Innovative designs of permafrost roadbed for the qinghai-tibet railway. *Sci. China Ser. E-Technol. Sci.* 52 (2), 530–538. doi:10.1007/s11431-008-0291-6

Chew, S. H., Kamruzzaman, A. H. M., and Lee, F. H. (2004). Physicochemical and engineering behavior of cement treated clays. *J. Geotech. Geoenviron. Eng.* 130 (7), 696–706. doi:10.1061/(asce)1090-0241(2004)130:7(696)

Consoli, N. C., Rosa, D. A., Cruz, R. C., and Rosa, A. D. (2011). Water content, porosity and cement content as parameters controlling strength of artificially cemented silty soil. *Eng. Geol.* 122 (3-4), 328–333. doi:10.1016/j.enggeo.2011.05.017

Daraei, A., Herki, B. M. A., Sherwani, A. F. H., and Zare, S. (2018). Slope stability in swelling soils using cement grout: A case study. *Int. J. Geosynth. Ground Eng.* 4, 10. doi:10.1007/s40891-018-0127-9

Ding, M. T., Zhang, F., Ling, X. Z., and Lin, B. (2018). Effects of freeze-thaw cycles on mechanical properties of polypropylene fiber and cement stabilized clay. *Cold Regions Sci. Technol.* 154, 155–165. doi:10.1016/j.coldregions.2018.07.004

JGJ (2011). *Specification for mix proportion design of cement soil*. Beijing, China: Ministry of housing and urban rural development of the people's republic of China.

Kang, G., Tsuchida, T., and Kim, Y. S. (2017). Strength and stiffness of cement-treated marine dredged clay at various curing stages. *Constr. Build. Mater.* 132, 71–84. doi:10.1016/j.conbuildmat.2016.11.124

Lai, Y. M., Pei, W. S., Zhang, M. Y., and Zhou, J. Z. (2014). Study on theory model of hydro-thermal-mechanical interaction process in saturated freezing silty soil. *Int. J. Heat Mass Transf.* 78, 805–819. doi:10.1016/j.ijheatmasstransfer.2014.07.035

Li, S. Y., Zhang, M. Y., Tian, Y. B., Pei, W. S., and Zhong, H. (2015). Experimental and numerical investigations on frost damage mechanism of a canal in cold regions. *Cold Regions Sci. Technol.* 116, 1–11. doi:10.1016/j.coldregions.2015.03.013

Lu, J. G., Pei, W. S., Zhang, X. Y., Bi, J., and Zhao, T. (2019b). Evaluation of calculation models for the unfrozen water content of freezing soils. *J. Hydrology* 575, 976–985. doi:10.1016/j.jhydrol.2019.05.031

Lu, J. G., Wan, X. S., Yan, Z. R., Pirhadi, N., Fan, X. Y., and Sun, M. N. (2022b). Hydro-thermal characteristics and deformation behaviors of silty clay subjected to freeze-thaw cycles. *Arab. J. Geosci.* 15, 446. doi:10.1007/s12517-022-09724-w

Lu, J. G., Wan, X. S., Yan, Z. R., Qiu, E. X., Pirhadi, N., and Liu, J. N. (2021). Modeling thermal conductivity of soils during a freezing process. *Heat. Mass Transf.* 575, 283–293. doi:10.1007/s00231-021-03110-0

Lu, J. G., Zhang, M. Y., and Pei, W. S. (2019a). Hydro-thermal behaviors of the ground under different surfaces in the qinghai-tibet plateau. *Cold Regions Sci. Technol.* 161, 99–106. doi:10.1016/j.coldregions.2019.03.002

Lu, J. G., Zhang, M. Y., Zhang, X. Y., Pei, W. S., and Bi, J. (2018). Experimental study on the freezing-thawing deformation of a silty clay. *Cold Regions Sci. Technol.* 151, 19–27. doi:10.1016/j.coldregions.2018.01.007

Lu, L. Y., Liu, C. H., Qu, S. Y., and Zhang, M. Z. (2022a). Experimental study on the mechanical and hydraulic behaviour of fibre-reinforced cemented soil with fly ash. *Constr. Build. Mater.* 321, 126374. doi:10.1016/j.conbuildmat.2022.126374

Lu, Y., Liu, S. H., Zhang, Y. G., Li, Z., and Xu, L. (2020). Freeze-thaw performance of a cement-treated expansive soil. *Cold Regions Sci. Technol.* 170, 102926. doi:10.1016/j.coldregions.2019.102926

Luis, A., Deng, L. J., Shao, L. S., and Li, H. Z. (2019). Triaxial behaviour and image analysis of edmonton clay treated with cement and fly ash. *Constr. Build. Mater.* 197, 208–219. doi:10.1016/j.conbuildmat.2018.11.222

Madhyannapu, R. S., and Puppala, A. J. (2014). Design and construction guidelines for deep soil mixing to stabilize expansive soils. *J. Geotech. Geoenviron. Eng.* 140 (9), 04014051. doi:10.1061/(ASCE)GT.1943-5606.0001149

Malekzadeh, M., and Bilsel, H. (2014). Hydro-mechanical behavior of polypropylene fiber reinforced expansive soils. *KSCE J. Civ. Eng.* 18 (7), 2028–2033. doi:10.1007/s12205-014-0389-2

Mardani-Aghabaglou, A., Kalıpcılar, İ., İnan Sezer, G., Sezer, A., and Altun, S. (2015). Freeze–thaw resistance and chloride-ion penetration of cement-stabilized clay exposed to sulfate attack. *Appl. Clay Sci.* 115, 179–188. doi:10.1016/j.clay.2015.07.041

Meng, T., Qiang, Y. J., Hu, A. F., Xu, C. T., and Lin, L. (2017). Effect of compound nano-$CaCO_3$ addition on strength development and microstructure of cement-stabilized soil in the marine environment. *Constr. Build. Mater.* 151, 775–781. doi:10.1016/j.conbuildmat.2017.06.016

Mengue, E., Mroueh, H., Lancelot, L., and Eko, R. M. (2018). Design and parametric study of a pavement foundation layer made of cement-treated fine-grained lateritic soil. *Soils Found.* 58 (3), 666–677. doi:10.1016/j.sandf.2018.02.025

Mujah, D., Rahman, M. E., and Zain, N. H. M. (2015). Performance evaluation of the soft soil reinforced ground palm oil fuel ash layer composite. *J. Clean. Prod.* 95, 89–100. doi:10.1016/j.jclepro.2015.02.058

Pei, W. S., Zhang, M. Y., Yan, Z. R., Lai, Y. M., Lu, J. G., and Dai, Y. J. (2022). Thermal control performance of the embankment with L-shaped thermosyphons and insulations along the gonghe-yushu highway. *Cold Regions Sci. Technol.* 194, 103428. doi:10.1016/j.coldregions.2021.103428

Qi, J. L., Ma, W., and Song, C. X. (2008). Influence of freeze-thaw on engineering properties of a silty soil. *Cold Regions Sci. Technol.* 53 (3), 397–404. doi:10.1016/j.coldregions.2007.05.010

Qi, J. L., Vermeer, P. A., and Cheng, G. D. (2006). A review of the influence of freeze-thaw cycles on soil geotechnical properties. *Permafr. Periglac. Process.* 17, 245–252. doi:10.1002/ppp.559

Qiu, G. Q., Liu, J. R., and Liu, H. X. (1994). *Geocryological glossary*. Lanzhou, China: Gansu Science and Technology Press.

Rezaeimalek, S., Huang, J., and Bin-Shafique, S. (2017). Evaluation of curing method and mix design of a moisture activated polymer for sand stabilization. *Constr. Build. Mater.* 146, 210–220. doi:10.1016/j.conbuildmat.2017.04.093

Taha, M. R. (2009). Geotechnical properties of soil-ball milled soil mixtures. *Nanotechnol. Constr.* 3, 377–382. doi:10.1007/978-3-642-00980-8_51

Taha, M. R., and Taha, O. M. E. (2012). Influence of nano-material on the expansive and shrinkage soil behavior. *J. Nanopart. Res.* 14 (10), 1190. doi:10.1007/s11051-012-1190-0

Tai, B. W., Liu, J. K., Wang, T. F., Shen, Y. P., and Li, X. (2017). Numerical modelling of anti-frost heave measures of high-speed railway subgrade in cold regions. *Cold Regions Sci. Technol.* 141, 28–35. doi:10.1016/j.coldregions.2017.05.009

Tang, C. S., Shi, B., and Zhao, L. Z. (2010). Interfacial shear strength of fiber reinforced soil. *Geotext. Geomembranes* 28, 54–62. doi:10.1016/j.geotexmem.2009.10.001

Topp, G. C., Davis, J. L., and Annan, A. P. (1980). Electromagnetic determination of soil water content: Measurements in coaxial transmission lines. *Water Resour. Res.* 16, 574–582. doi:10.1029/WR016i003p00574

Wang, C., Li, S, Y., Chen, Q., Zhang, H., Liu, X. Y., and Ren, X. C. (2021). Statistical studies on the pore characteristic of qinghai-tibet plateau silty clay modified by nano-silica. *Microporous Mesoporous Mater.* 322, 111175. doi:10.1016/j.micromeso.2021.111175

Wang, F. T., Li, K. Q., and Liu, Y. (2022). Optimal water-cement ratio of cement-stabilized soil. *Constr. Build. Mater.* 320, 126211. doi:10.1016/j.conbuildmat.2021.126211

Wei, L., Chai, S. X., Zhang, H. Y., and Shi, Q. (2018). Mechanical properties of soil reinforced with both lime and four kinds of fiber. *Constr. Build. Mater.* 172, 300–308. doi:10.1016/j.conbuildmat.2018.03.248

Xue, Y. G., Kong, F. M., Li, S. C., Zhang, Q. S., Qiu, D. H., Su, M. X., et al. (2021). China starts the world's hardest "sky-high road" project: Challenges and countermeasures for sichuan-tibet railway. *Innovation* 2 (2), 100105. doi:10.1016/j.xinn.2021.100105

Yi, Y. L., Liu, S. Y., and Puppala, A. J. (2018). Bearing capacity of composite foundation consisting of T-shaped soil-cement column and soft clay. *Transp. Geotech.* 15, 47–56. doi:10.1016/j.trgeo.2018.04.003

Yu, H., Yi, Y. L., Romagnoli, A., and Tan, W. L. (2022). Cement soil stabilization for underground liquid natural gas storage. *Cold Regions Sci. Technol.* 194, 103438. doi:10.1016/j.coldregions.2021.103438

Zhang, M. Y., Lu, J. G., Lai, Y. M., and Zhang, X. Y. (2018a). Variation of the thermal conductivity of a silty clay during a freezing-thawing process. *Int. J. Heat Mass Transf.* 124, 1059–1067. doi:10.1016/j.ijheatmasstransfer.2018.02.118

Zhang, M. Y., Lu, J. G., Pei, W. S., Lai, Y. M., Yan, Z. R., and Wan, X. S. (2021). Laboratory study on the frost-proof performance of a novel embankment dam in seasonally frozen regions. *J. Hydrology* 602, 126769. doi:10.1016/j.jhydrol.2021.126769

Zhang, M. Y., Pei, W. S., Lai, Y. M., Niu, F. J., and Li, S. Y. (2017). Numerical study of the thermal characteristics of a shallow tunnel section with a two-phase closed thermosyphon group in a permafrost region under climate warming. *Int. J. Heat Mass Transf.* 104, 952–963. doi:10.1016/j.ijheatmasstransfer.2016.09.010

Zhang, X. Y., Zhang, M. Y., Pei, W. S., and Lu, J. G. (2018b). Experimental study of the hydro-thermal characteristics and frost heave behavior of a saturated silt within a closed freezing system. *Appl. Therm. Eng.* 129, 1447–1454. doi:10.1016/j.applthermaleng.2017.10.116

Zhang, Y., Johnson, A. E., and White, D. J. (2019). Freeze-thaw performance of cement and fly ash stabilized loess. *Transp. Geotech.* 21, 100279. doi:10.1016/j.trgeo.2019.100279